Imaging dopamine D_3 receptors in the human brain with Positron Emission Tomography, [^{11}C]PHNO, and a selective D_3 receptor antagonist.

Graham Searle[1], John D. Beaver[1], Robert A. Comley[1], Massimo Bani[2], Andri Tziortzi[1], Mark Slifstein[3], Manolo Mugnaini[2], Cristiana Griffante[2], Alan A. Wilson[4], Emilio Merlo-Pich[2], Sylvain Houle[4], Roger Gunn[1,5,6], Eugenii A. Rabiner[1,6], Marc Laruelle[1,2,3,6]

1. Clinical Imaging Centre, GlaxoSmithKline, London, U.K.

2. Neurosciences Centre of Excellence in Drug Discovery, GlaxoSmithKline, Verona, Italy

3. Department of Psychiatry, Columbia University, New York, USA

4. Centre for Addiction and Mental Health, Toronto, Canada

5. Department of Engineering Science, University of Oxford, U.K.

6. Division of Neuroscience and Mental Health, Imperial College, London, U.K.

Corresponding author contact details:

Graham Searle

GlaxoSmithKline Clinical Imaging Centre

Imperial College London, Hammersmith Hospital

Du Cane Road

London W12 0NN

UK

Email: graham.e.searle@gsk.com

Tel: +44(0)20 8008 6049 Fax: +44(0)20 8008 6491

Number of words in abstract: 250; words in text: 4000. Number of tables: 2; figures: 6. No supplementary material.

ABSTRACT

Background: Dopamine D_3 receptors are involved in the pathophysiology of several neuropsychiatric conditions. [^{11}C]-(+)-PHNO is a radiolabelled D_2 and D_3 agonist, suitable for imaging the agonist binding sites (denoted D_{2HIGH} and D_3) of these receptors with Positron Emission Tomography (PET). PET studies in nonhuman primates documented that, in vivo, [^{11}C]-(+)-PHNO displays a relative selectivity for D_3 compared to D_{2HIGH} receptor sites, and that the [^{11}C]-(+)-PHNO signal is enriched in D_3 contribution compared to conventional ligands such as [^{11}C]raclopride.

Methods: To define the D_3 contribution (f_{PHNO}^{D3}) to [^{11}C]-(+)-PHNO binding potential (BP_{ND}) in healthy humans, fifty-two scans were obtained in nineteen healthy volunteers, at baseline and following oral administration of various doses of the selective D_3 receptor antagonist, GSK598809.

Results: The impact of GSK598809 on [^{11}C]-(+)-PHNO was regionally selective. In dorsal regions of the striatum, GSK598809 did not significantly affect [^{11}C]-(+)-PHNO BP_{ND} ($f_{PHNO}^{D3} \approx 0\%$). Conversely, in the substantia nigra (SN), GSK598809 dose-dependently reduced [^{11}C]-(+)-PHNO binding to nonspecific level ($f_{PHNO}^{D3} \approx 100\%$). In ventral striatum (VST), globus pallidus (GP) and thalamus (THA), [^{11}C]-(+)-PHNO BP_{ND} was attributable to a combination of D_{2HIGH} and D_3 receptor sites, with f_{PHNO}^{D3} of 26%, 67% and 46%, respectively. D_3 receptor binding potential (BP_{ND}^{D3}) was highest in GP (1.90) and SN (1.39), with lower levels in VST (0.77) and THA (0.18) and negligible levels in dorsal striatum.

Conclusions: This study elucidated the pharmacological nature of the [^{11}C]-(+)-PHNO signal in healthy subjects, and provided the first quantification of D_3 receptor availability with PET in the living human brain.

Clinical trial details: “Study of Safety, Blood Levels and Brain Receptor Occupancy of GSK598809 Using PET Imaging in Health Males.”; clinicaltrial.gov identifier: NCT00468806.

URL: http://www.clinicaltrial.gov/ct2/show/NCT00468806

INTRODUCTION

Dopamine (DA) D_3 receptors are members of the DA D_2-like receptor family and are involved in functions mediated by the mesolimbic dopaminergic system, including reward and reinforcement. A substantial body of literature supports the role of D_3 receptors in the pathophysiology of several conditions such as addiction, schizophrenia and Parkinson's disease (PD) and a number of D_3 receptor agents are currently under development (1-4).

Advances in the understanding of the role of D_3 receptors in neuropsychiatric conditions have been limited by the lack of a method to measure D_3 receptors in the living human brain. Radiotracers commonly used to image D_2-like receptors with Positron Emission Tomography (PET), such as [^{11}C]raclopride, [^{18}F]fallypride or [^{11}C]FLB457 are antagonists that display similar affinity for D_2 and D_3 receptors (5-7). These receptors co-localize in brain regions where the density of D_3 receptors is generally lower than that of D_2 receptors. Therefore, the D_3 receptor contribution to the signal of these conventional radiotracers tends to be quite small. Efforts to develop selective D_3 receptor PET radiotracers have so far been unsuccessful.

The demonstration of the in vivo D_3 receptor preferring properties of the recently developed D_2-like agonist PET radiotracer [^{11}C]-(+)-4-propyl-3,4,4a,5,6,10b-hexahydro-2H-naphtho[1,2-b][1,4]oxazin-9-ol ([^{11}C]-(+)-PHNO) opened up the possibility to image D_3 receptors with PET (8). (+)-PHNO was first reported as a potent D_2 agonist intended for the treatment of PD (9). Initial evaluation of [^{11}C]-(+)-PHNO in vivo binding in rats showed that [^{11}C]-(+)-PHNO was a suitable agonist radiotracer to measure D_2-like agonist receptor sites in the striatum (10). Examination of [^{11}C]-(+)-PHNO in vivo binding in humans demonstrated the expected high specific signal in the striatum, but revealed an unexpectedly high accumulation in the ventral striatum and globus pallidus compared to [^{11}C]raclopride (11). PET studies in baboons demonstrated that the enriched [^{11}C]-(+)-PHNO signal in these regions was selectively decreased by pretreatment with the D_3 receptor partial agonist BP-897, suggesting that the difference in regional distributions between [^{11}C]raclopride and [^{11}C]-(+)-PHNO was driven by

a relatively higher affinity of this tracer for D_3 compared to D_{2HIGH} receptor sites (8). This finding was consistent with data from most but not all in vitro affinity studies (see Table 1 in 8). This proposition was recently confirmed by examining the effect of pretreatment with the selective D_3 antagonist SB-277011 (100-fold selectivity for D_3 over D_2 in vitro) on in vivo [^{11}C]-(+)-PHNO binding in baboons (12).

While the [^{11}C]-(+)-PHNO in vivo signal is enriched in D_3 versus D_2 receptor contributions, selective pharmacological blockade is required to differentiate these components. Here, we report the in vivo distribution of [^{11}C]-(+)-PHNO in the human brain, at baseline and after administration of various ascending doses of the selective D_3 receptor antagonist GSK598809 (13)(in vitro K_i of 6.2 and 740 nM against [^{3}H]-PHNO in filtration binding experiments on membranes obtained from Chinese hamster ovary (CHO) cells expressing human D_3 and D_2 receptors, respectively). Fifty two [^{11}C]-(+)-PHNO scans were obtained in nineteen subjects, at baseline and after various doses of GSK598809. Comparison of [^{11}C]-(+)-PHNO binding at baseline and following D_3 receptor blockade enabled dissection of the D_{2HIGH} and D_3 receptor components of the [^{11}C]-(+)-PHNO regional specific binding and quantification of regional D_3 receptor binding potential in the living human brain.

MATERIAL AND METHODS

General design

The study was approved by the Centre for Addiction and Mental Health (CAMH) Research Ethics Board and performed at the CAMH PET Centre, Toronto. The study was sponsored by GlaxoSmithKline and the protocol was posted on clinicaltrial.gov (identifier NCT00468806) prior to study initiation. Nineteen healthy volunteers were included in the study. Each subject received a baseline [^{11}C]-(+)-PHNO scan and one to three [^{11}C]-(+)-PHNO scans following administration of one to three oral doses of GSK598809 (range from 5 to 175 mg). The post-challenge PET scans were scheduled to begin around two to three hours after administration in order to estimate occupancy shortly after the anticipated plasma peak. Blood

samples were taken for analysis of GSK598809 pharmacokinetics.

Subjects

Inclusion criteria were: male non-smokers aged between 22 and 55 years old, with body mass index (BMI) between 19.0 – 29.0 kg/m^2 and the absence of past or present neurological, medical, or psychiatric illnesses and concomitant medications. Clinical status was assessed by history, review of systems, physical examination, routine blood tests, urine toxicology and EKG. Subjects provided written informed consent.

Radiochemistry

Radiosynthesis of [^{11}C]-(+)-PHNO was performed as previously described (10). Briefly, [^{11}C]propionylchloride was reacted with 9-hydroxynaphthoxazine to generate a [^{11}C]amide, which was subsequently reduced by lithium aluminium hydride. Purification by HPLC and formulation gave radiochemically pure [^{11}C]-(+)-PHNO as a sterile, pyrogen-free solution suitable for human studies.

PET protocol

Dynamic PET scans were acquired using a Siemens Biograph 16 HI-REZ PET-CT (Siemens Healthcare) in 3D mode. A CT scan was acquired for attenuation correction of PET data prior to administration of the radiotracer. The radiotracer was then administered as an intravenous bolus over 30 seconds, and dynamic PET data were acquired for 90 minutes. The PET data were binned into 26 frames (durations: 8 x 15s, 3 x 60s, 5 x 2min, 5 x 5min, 5 x 10min) and reconstructed using Fourier rebinning and 2D filtered back projection with a ramp filter at Nyquist cut-off frequency. Image data were smoothed with a Gaussian filter (5 mm FWHM). Arterial sampling for measurement of [^{11}C]-(+)-PHNO input function was not performed. A T1-weighted image (FSPGR sequence) was also acquired for each subject using a GE Signa Excite HD 1.5T scanner system (GE Healthcare, U.S.A.).

Image analysis

Scans were analyzed at the Clinical Imaging Centre, GlaxoSmithKline, London. Dynamic PET images were registered to the subject's MR image, and corrected for motion using

a frame-to-frame registration process with a mutual information cost function.

Six regions of interests (ROI) were analyzed: ventral striatum (VST), dorsal caudate (DCA), dorsal putamen (DPU), globus pallidus (GP), thalamus (THA) and substantia nigra (SN). VST, DCA, DPU, GP and THA were defined manually on each subject's MR image (14). SN was defined manually on each subject's baseline PET integral image. The cerebellum (CER) was defined via nonlinear registration (using SPM5b; Wellcome Trust Centre for Neuroimaging, http://www.fil.ion.ucl.ac.uk/spm) of a template MR image and corresponding brain atlas. Each ROI was then applied to the dynamic PET data to derive regional time-activity curves.

[^{11}C]-(+)-PHNO binding potential

The binding potential relative to the nondisplaceable compartment (BP_{ND}) is equal to the product of receptor density ($B_{\max}$), affinity of ligand for the target ($1/K_D$) and the free fraction in the brain (f_{ND}):

$$BP_{ND} = \frac{f_{ND} B_{\max}}{K_D}. \quad (1)$$

D_2 receptors are configured in interconvertible states of high (D_{2HIGH}) and low (D_{2LOW}) affinity for agonists (15-17). At the doses used in this study, the agonist [^{11}C]-(+)-PHNO is expected to bind only to D_{2HIGH} receptors. In contrast, D_3 receptors appear to be essentially configured in a single high affinity state for agonists (see references and discussion in (12)). Thus [^{11}C]-(+)-PHNO BP_{ND} can be decomposed:

$$\begin{aligned} BP_{ND} &= BP_{ND}^{D3} + BP_{ND}^{D2HIGH} \\ &= f_{ND}\left(\frac{B_{\max}^{D3}}{K_D^{D3}} + \frac{B_{\max}^{D2HIGH}}{K_D^{D2HIGH}}\right), \end{aligned} \quad (2)$$

where BP_{ND}^{D3} and BP_{ND}^{D2HIGH} are the BP_{ND} for D_3 and D_{2HIGH} receptor sites, respectively.

Quantitative analysis was performed using the simplified reference tissue model (SRTM, (18)) , with cerebellum as reference region, to derive regional estimates of BP_{ND} . Model fits and parameter estimates were obtained via the basis function implementation (19). The occupancy of [^{11}C]-(+)-PHNO induced by GSK598809 was quantified by relating BP_{ND} measured in the presence of GSK598809 ($BP_{ND\ GSK\,598809}$) to baseline BP_{ND} ($BP_{ND\ Baseline}$):

$$Occupancy = \frac{BP_{ND\ Baseline} - BP_{ND\ GSK\ 598809}}{BP_{ND\ Baseline}}. \quad (3)$$

Fraction of [^{11}C]-(+)-PHNO BP_{ND} corresponding to binding to D_3 receptor (f_{PHNO}^{D3})

The fraction of baseline [^{11}C]-(+)-PHNO BP_{ND} corresponding to binding to D_3 receptors (f_{PHNO}^{D3}) is:

$$f_{PHNO}^{D3} = \frac{BP_{ND}^{D3}}{BP_{ND}^{D3} + BP_{ND}^{D2HIGH}}, \quad (4)$$

where BP_{ND}^{D3} and BP_{ND}^{D2HIGH} are the baseline [^{11}C]-(+)-PHNO binding potentials at the D_3 and D_{2HIGH} sites respectively. Occupancy by GSK598809 can be described by:

$$Occupancy = f_{PHNO}^{D3}\left(\frac{C_P^{GSK\,598809}}{C_P^{GSK\,598809} + EC_{50}^{D3}}\right), \quad (5a)$$

where $C_P^{GSK\,598809}$ is the GSK598809 total plasma concentrations at the beginning of the scan, and EC_{50}^{D3} is the total plasma concentration of GSK598809 associated with 50% occupancy of brain D_3 receptors. In terms of BP_{ND}, this relationship is:

$$BP_{ND}^{Measured} = BP_{ND}^{Baseline}\left(\frac{f_{PHNO}^{D3}}{1 + \frac{C_P^{GSK\,598809}}{EC_{50}^{D3}}} + \left(1 - f_{PHNO}^{D3}\right)\right), \quad (5b)$$

where $BP_{ND}^{Baseline}$ is baseline BP_{ND} and $BP_{ND}^{Measured}$ is the BP_{ND} measured in any given scan.

Regional f_{PHNO}^{D3} were estimated via model fits to all data from all ROIs simultaneously using Equation 5b. The parameter EC_{50}^{D3} was shared between regions, while each region had its own f_{PHNO}^{D3}. This analysis assumes that the affinity of GSK598809 for D_3 receptors is invariant across regions and across subjects. The estimation of regional f_{PHNO}^{D3} permitted the calculation of BP_{ND}^{D3} and BP_{ND}^{D2HIGH} values using Equation 4.

This analysis also assumes that, at doses used in this study, GSK598809 binding to D_2 receptors was negligible. To check this assumption, data were also analyzed using a two site model which accounted for possible occupancy of D_2 receptors by GSK598809:

$$Occupancy = f_{PHNO}^{D3}\left(\frac{C_P^{GSK\,598809}}{C_P^{GSK\,598809} + EC_{50}^{D3}}\right) + \left(1 - f_{PHNO}^{D3}\right)\left(\frac{C_P^{GSK\,598809}}{C_P^{GSK\,598809} + EC_{50}^{D2}}\right), \quad (6a)$$

and

$$BP_{ND}^{Measured} = BP_{ND}^{Baseline}\left(\frac{f_{PHNO}^{D3}}{1+\frac{C_P^{GSK\,598809}}{EC_{50}^{D3}}}+\frac{\left(1-f_{PHNO}^{D3}\right)}{1+\frac{C_P^{GSK\,598809}}{EC_{50}^{D2}}}\right), \quad (6b)$$

where EC_{50}^{D2} is the plasma concentration of GSK598809 associated with 50% occupancy D_2 receptors.

RESULTS

Summary scan data

A total of 52 [^{11}C]-(+)-PHNO scans were obtained in 19 subjects (19 baseline scans and 33 scans following administration of GSK598809). Doses used were 5 mg (3 scans), 25 mg (4 scans), 50 mg (3 scans), 75 mg (14 scans), 130 mg (2 scans) and 175 mg (7 scans). Subject ages were 36.2 ± 9.6 years (mean ± SD) and BMI was 25.1 ± 2.4 kg/m^2. Eight subjects received two scans (one baseline and one after GSK598809 administration), eight subjects received three scans (baseline plus two scans after GSK598809 administrations) and three subjects received four scans (one baseline plus three scans after GSK598809 administrations). [^{11}C]-(+)-PHNO injected doses were 298 ± 50.3 MBq. [^{11}C]-(+)-PHNO injected masses were 2.36 ± 0.13 micrograms. For the post-GSK598809 scans, the interval between GSK598809 administration and [^{11}C]-(+)-PHNO injections was 2.8 ± 1.5 hours. For each subject, administrations of GSK598809 were separated by at least one week.

Baseline scans

Figure 1 shows a representative PET image (imaged summed over 10-90 min.), with coregistered MRI, showing the regional distribution of [^{11}C]-(+)-PHNO uptake in the human brain. High accumulation is observed in the striatal regions, GP and SN, and low levels in THA, CER and cortical regions. [^{11}C]-(+)-PHNO time activity curves and SRTM model fits under baseline conditions in one representative subject are presented in Figure 2a. CER, THA and the striatal regions (VST, DCA and DPU) peaked early and displayed rapid wash-out. In GP and SN, the washout was more protracted. The SRTM was found to describe the tissue data well. Figure 3 summarises the calculated baseline [^{11}C]-(+)-PHNO BP_{ND} in the 19 subjects.

Scans following GSK598809 administration

Figure 4 shows representative [^{11}C]-(+)-PHNO scans (imaged summed over 10-90 min.) at baseline (top) and after administration of 175 mg GSK598809 (bottom). Slices were selected to illustrate the marked change in SN, moderate change in GP and VS, and marginal change in dorsal striatal regions following D_3 receptor blockade. Figure 2b shows [^{11}C]-(+)-PHNO time activity curves and SRTM model fits after administration of 175 mg GSK598809 in the same subject as depicted in Figure 2a. GSK598809 (175 mg) administration reduced [^{11}C]-(+)-PHNO uptake in SN to levels comparable to the cerebellum. The uptake was also significantly reduced in the GP. Activities in dorsal striatal regions were unaffected.

Derivation of f_{PHNO}^{D3}

The model described in Equation 5b was fitted to all subjects and all regions simultaneously. Data and model fits are shown in Figure 5. The two site model (Equation 6b) was also fitted to the data. No significant improvement in model fit was produced and consideration of the Akaike Information Criterion (1-site: -810, 2-site: -809) indicated that the single site model was most appropriate. Furthermore, estimation of f_{PHNO}^{D3} by Equation 5b and Equation 6b yielded nearly identical results. Thus, only results of the one site model are presented here.

Examination of the effects of GSK598809 on [^{11}C]-(+)-PHNO BP_{ND} revealed marked differences between regions. High GSK598809 plasma concentrations were associated with almost complete blockade of [11C]-(+)-PHNO specific binding in SN, and little detectable changes in the dorsal regions of the striatum. Model fit results with confidence intervals are given in Table 1. The lack of effect of GSK598809 in DCA and DPU resulted in f_{PHNO}^{D3} close to zero. In contrast, f_{PHNO}^{D3} in SN was close to 100%. VST, GP and THA produced intermediate values, with f_{PHNO}^{D3} of 0.26, 0.67 and 0.46, respectively. Regional f_{PHNO}^{D3} estimates permitted the calculation of BP_{ND}^{D3} and BP_{ND}^{D2HIGH} in each region (Table 1 and Figure 6). The highest concentration of D_3 receptors were found in GP (BP_{ND}^{D3} of 1.90), followed by SN (BP_{ND}^{D3} of 1.39), with lower levels in VST (BP_{ND}^{D3} of 0.77) and THA (BP_{ND}^{D3} of 0.18).

DISCUSSION

Technical limitations

Technical limitations of this study should be acknowledged. No arterial input function was measured, and the SRTM was used to derive BP_{ND}. The SRTM is known to underestimate BP_{ND} in regions of high binding when the reference region does not follow a one compartment model in response to the true input function (20). Full quantitative analysis of [^{11}C]-(+)-PHNO uptake using arterial input function suggested that this could be the case for this tracer (21). This effect could lead to a small underestimation of occupancy in high density regions, but would not change the main conclusions of this study.

A second limitation resulting from the lack of input function measurement is the absence of quantification of the effects of GSK598809 on cerebellum distribution volume. Like previous investigators, we considered the cerebellum as an appropriate region of reference, i.e. devoid of significant amounts of D_3 receptors (11, 21-24). However, on examination of cerebellar standard uptake values (SUVs, i.e. regional activity normalized by injected dose and body weight), a small dose dependent decrease in cerebellum SUVs was observed. At the highest achieved D_3 receptor blockade (175 mg dose), cerebellum SUVs decreased by about 30% in the late phase of the scans. Such an effect could be due to changes in input function, to the presence of D_3 receptors in cerebellum or to some combination of both factors. This observation contrasts with the reported lack of effect of haloperidol on [^{11}C]-(+)-PHNO cerebellum SUVs in humans (11). There the small number of subjects examined (three) may have produced inadequate sensitivity to detect an effect. Our observations were consistent with the decrease in [^{11}C]-(+)-PHNO cerebellum distribution volumes reported in baboons following administration of high doses of SB-277011 (12). This effect could lead to a slight underestimation of regional f_{PHNO}^{D3}, but would not affect the main conclusions of this study. The possibility of signal contamination from adjacent regions (such as the vermis) was checked via definition of subdivisions of the cerebellar ROI. Consistent changes in SUV values in cortical regions were also found,

suggesting that the effect cannot be attributed to inappropriate definition of the reference region. Studies with input function measurement, D_3 receptor blockade and full quantitative analysis in humans are warranted to examine these issues.

A further potential technical limitation relates to the definitions of the target-rich ROIs used. Some of the regions considered are small and thus potentially sensitive to subject motion and image registrations. Striatal regions such as DPU and GP lie close to each other and so there is some potential for spillover of signal between regions. The GP is also possibly heterogenous in distribution of D_2 and D_3 receptors (25), and has somewhat indistinct boundaries on T1 MRI images. This could increase variability in outcome parameters.

Comparison with other data sets

The fact that the differences between the in vivo regional distributions of [^{11}C]-(+)-PHNO and [^{11}C]raclopride are primarily due to the preferential affinity of [^{11}C]-(+)-PHNO for D_3 receptors was first demonstrated in baboons, using the D_3 partial agonist BP897 (3 baboons, six scans, single dose of 0.25 mg/kg, i.v., Table 2) (8). The larger reduction in [^{11}C]-(+)-PHNO BP_{ND} compared to [^{11}C]raclopride BP_{ND} induced by BP897 showed that [^{11}C]-(+)-PHNO was more selective than [^{11}C]raclopride for D_3 receptors. These results were confirmed in baboons using the highly selective D_3 receptor antagonist SB-277011, and a dose-response curve method similar to that used here (3 baboons, 18 scans, 0.5, 2 and 5 mg/kg i.v., Table 2) (12). A baboon study was also carried out with GSK598809 (3 baboons, 16 PET scans, dose range 0.1 to 1 mg/kg i.v., unpublished data, Table 2). Regional f_{PHNO}^{D3} values measured with GSK598809 in baboons were similar to those derived with SB-277011. The results reported in this study are consistent with the baboon data, in the general magnitude and rank order of regional f_{PHNO}^{D3} (SN> GP> THA> VST> DCA> DPU). The f_{PHNO}^{D3} obtained here for thalamus (46%) is somewhat lower than those reported in baboon studies (60% - 97%). However, as a result of the low [^{11}C]-(+)-PHNO binding potential in thalamus and consequently noisy data, our confidence interval for thalamus spans the full range from zero to one. Thus this difference should not be considered significant.

The results of this study differ with the results of a [^{11}C]-(+)-PHNO occupancy study in humans with ABT-925, an antagonist with 50-100 fold selectivity for the D_3 over the D_2 in vitro (23). ABT-925 reduced [^{11}C]-(+)-PHNO BP_{ND} by a relatively large and comparable amount in both dorsal and ventral regions of the striatum (Table 2). Here, the 175 mg dose of GSK598809 had very little effect in dorsal striatum, while inducing nearly 100% displacement in the SN. These discrepant findings may be accounted for by a lower D_3/D_2 selectivity of ABT-925 compared to GSK598809 in vivo. A two site fit of the in vivo ABT-925 data indicated only a 2-4 fold selectivity for D_3 over D_2 (23). This suggestion is supported by results of in vitro ^{35}S-GTPγS functional inhibition studies against quinelorane on membranes obtained from CHO cells expressing human D_3 and D_2 receptors (according to the method described in (13), where ABT-925 exhibited fpK_i values of 8.19 and 7.01 at D_3 and D_2 receptors, respectively (about 15 fold selectivity)), while GSK598809 exhibited fpK_i values of 8.9 and 6.2, at D_3 and D_2 receptors, respectively (about 500 fold selectivity).

D_3 and D_2 receptor distribution

The lack of detectable D_3 receptor signal in the dorsal striatum is consistent with the low levels of expression of these receptors documented in human postmortem studies. Seeman et al. (26) failed to detect any D_3 receptor binding in dorsal regions of the human striatum, whilst other investigators detected low levels of D_3 receptors in dorsal striatum (25, 27). This study does not, however, rule out the existence of low levels of D_3 receptors in the striatum, which could have been obscured by the technical limitations discussed above.

Significant concentrations of D_3 receptors were detected in VST, GP and SN, regions where high expression of D_3 receptors have been documented postmortem (25, 27). The fraction of observed PHNO signal in GP attributed here to D_3 (67%) is somewhat higher than the value of 35% determined in the autoradiographic studies of Seeman et al. (26), though consistent with other in vivo experiments (see Table 2). This disparity could be due to differences between the in vitro and in vivo settings. It has been suggested that [^{11}C]-(+)-PHNO binding to D_3 receptors in the GP can increase in response to long term administration of D_2 antagonists (28), however a

similar effect here is considered unlikely since GSK598809 was administered acutely. The presence of D_3 receptors in SN is compatible with their proposed function as autoreceptors, although the majority of D_3 receptors in the SN may not be located on DA cells (29-30). Interestingly, in Parkinson's patients, [^{11}C]-(+)-PHNO binding in the SN is not decreased, supporting the notion that the majority of D_3 receptors in that area are not located on DA cells (22).

The lack of detection of D_{2HIGH} receptors in SN with [^{11}C]-(+)-PHNO might seem surprising given the well documented presence of D_2 receptors in SN. However, it should be remembered that the measured PET signal (BP_{ND}) is proportional to $B_{\max}/K_D$. Thus if the ligand has different affinities for the two binding sites then the fraction f_{PHNO}^{D3} of BP_{ND} corresponding to D_3 binding can be very different from the D_3 fraction of receptor concentration ($f_{B\max}^{D3}$). The in vivo affinities of [^{11}C]-(+)-PHNO for D_3 and D_{2HIGH} receptors were recently measured in rhesus monkeys using PET and a two site model (31). The potency of (+)-PHNO to block [^{11}C]-(+)-PHNO was about 20-fold higher in SN compared to dorsal striatum, indicating a 20-fold in vivo selectivity (K_D^{D2HIGH}/K_D^{D3}) of [^{11}C]-(+)-PHNO for D_3 compared to D_{2HIGH}. Given this level of selectivity, it is entirely plausible that a region could have a substantial fraction $f_{B\max}^{D2HIGH}$, yet a small contribution of D_{2HIGH} receptors to [^{11}C]-(+)-PHNO BP_{ND}. If we suppose that the same 20-fold in vivo selectivity exists in human, then Equation 4 can be rewritten as

$$f_{PHNO}^{D3} = \frac{B_{\max}^{D3}}{B_{\max}^{D3} + 0.05B_{\max}^{D2HIGH}}. \quad (7)$$

Baboon PET experiments with [^{18}F]fallypride (32) and human in vitro experiments (25, 27) suggest that around 40% of the D_2-like receptors in SN are D_3. Applying Equation 7, a 40% D_3 receptor concentration fraction could be expected to translate into a f_{PHNO}^{D3} value of around 95%, consistent with the results presented here. Further PET experiments in humans using GSK598809 and a radioligand such as [^{18}F]fallypride could be employed to obtain a more precise estimate of the relative densities of D_2 and D_3 receptors in the SN.

Implications for imaging studies

The results of this study have implications for future imaging studies with [^{11}C]-(+)-PHNO. First, at a time when several selective D_3 receptor antagonists and "optimized" D_3/D_2 receptor antagonists are under development (1-3), [^{11}C]-(+)-PHNO scans in healthy volunteers provide a simple method to simultaneously quantify the in vivo occupancy at both D_3 and D_2 receptors by examining the decrease in [^{11}C]-(+)-PHNO BP_{ND} in SN and dorsal striatum, respectively.

Second, this study informs the emerging literature reporting the distribution of [^{11}C]-(+)-PHNO BP_{ND} in pathological conditions. For example, Graff-Guerrero et al. (24) reported unchanged [^{11}C]-(+)-PHNO BP_{ND} in drug-free patients with schizophrenia, a result that might seem at variance with the postmortem finding of significant upregulation of D_3 receptors in VST in schizophrenia (33). However, since only about 26% of VST [^{11}C]-(+)-PHNO BP_{ND} corresponds to binding to D_3 receptors, such an upregulation, if present, might have been obscured by the mixed nature of the VST [^{11}C]-(+)-PHNO signal. Boileau et al. (22) studied [^{11}C]-(+)-PHNO and [^{11}C]raclopride distributions in PD patients. Regions were classified as D_3 "rich" (VST and GP) or D_2 receptor "rich" (DCA and DPU). In PD subjects, [^{11}C]raclopride and [^{11}C]-(+)-PHNO BP_{ND} 's were increased in DPU, [^{11}C]-(+)-PHNO but not [^{11}C]raclopride BP_{ND} 's were decreased in GP, and both ligands were unaffected in the VST. The authors interpreted the results as demonstrating an upregulation of D_2 receptors in DPU and a downregulation of D_3 receptors in GP, an interpretation that is in line with the results of the present study. It is unclear if the lack of findings in the VST is due to this region being relatively unaffected in PD, or to the fact that D_3 receptors contribute only a small fraction of [^{11}C]-(+)-PHNO specific binding in VST. Future studies with [^{11}C]-(+)-PHNO aiming at characterizing D_{2HIGH} and D_3 distributions with [^{11}C]-(+)-PHNO in mixed regions (VST, GP, THA) will benefit from the combination of a baseline scan with a scan obtained following administration of a selective D_3 receptor antagonist. This would be especially important in the study of addictive conditions, where D_2 and D_3 receptors have been showed to be decreased and increased,

respectively (reviewed in (4, 34)).

CONCLUSIONS

In conclusion, this study elucidated the pharmacological nature of the [^{11}C]-(+)-PHNO signal in healthy subjects, and provided quantification of D_3 receptor availability in the living human brain. The [^{11}C]-(+)-PHNO signal was found to be relatively selective for D_{2HIGH} in DCA and DPU, and for D_3 in SN, while it was mixed in VST, GP and THA. The highest concentration of D_3 receptors were found in GP (BP_{ND}^{D3} of 1.90), followed by SN (BP_{ND}^{D3} of 1.39), with lower levels in VST (BP_{ND}^{D3} of 0.77) and THA (BP_{ND}^{D3} of 0.18). Given the relatively selective nature of the [^{11}C]-(+)-PHNO signal in DCA, DPU and SN, [^{11}C]-(+)-PHNO can be used to measure drug-induced occupancy at both D_{2HIGH} and D_3 receptors in healthy volunteers. In the absence of truly selective D_2 or D_3 PET radioligands, the combination of [^{11}C]-(+)-PHNO and a selective D_3 receptor antagonist provides a method for dissecting D_3 and D_{2HIGH} receptor availability in mixed regions such as VST and GP. The ability to measure D_3 receptors in health and disease, as well as the level of engagement of this target by therapeutic agents, will be very valuable to unravel the role of D_3 receptors in the pathophysiology and treatment of neuropsychiatric conditions.

ACKNOWLEDGEMENTS

This study was funded by GlaxoSmithKline. The authors acknowledge the contributions from the GSK598809 project team, with special thanks to Stephen Mark, and from the staff of the Centre for Addiction and Mental Health PET Centre in Toronto, of the GSK Clinical Imaging Centre in London, and of GSK Screening and Compound Profiling in Harlow.

Financial Disclosure

G.S., J.B., R.C., M.B., A. T., M.M., C.G., E.M.-P., R.G., E.R. and M.L. are employees of GSK.

M.S., A.W., and S.H. are recipients of research funding from GSK.

REFERENCES

1. Joyce JN, Millan MJ (2005): Dopamine D3 receptor antagonists as therapeutic agents. *Drug Discov Today*. 10:917-925.
2. Sokoloff P, Diaz J, Le Foll B, Guillin O, Leriche L, Bezard E, et al. (2006): The dopamine D3 receptor: a therapeutic target for the treatment of neuropsychiatric disorders. *CNS Neurol Disord Drug Targets*. 5:25-43.
3. Millan MJ, Brocco M (2008): Cognitive Impairment in Schizophrenia: a Review of Developmental and Genetic Models, and Pro-cognitive Profile of the Optimised D3>D2 Antagonist, S33138. *Thérapie*. 63:187-229.
4. Heidbreder CA, Gardner EL, Xi ZX, Thanos PK, Mugnaini M, Hagan JJ, et al. (2005): The role of central dopamine D3 receptors in drug addiction: a review of pharmacological evidence. *Brain Res Brain Res Rev*. 49:77-105.
5. Halldin C, Farde L, Hogberg T, Mohell N, Hall H, Suhara T, et al. (1995): Carbon-11-FLB 457: A Radioligand for Extrastriatal D2 Dopamine Receptors. *J Nucl Med*. 36:1275-1281.
6. Levant B, Grigoriadis DE, De Souza EB (1995): Relative affinities of dopaminergic drugs at dopamine D2 and D3 receptors. *European Journal of Pharmacology*. 278:243-247.
7. Mukherjee J, Yang Z-Y, Brown T, Lew R, Wernick M, Ouyang X, et al. (1999): Preliminary assessment of extrastriatal dopamine d-2 receptor binding in the rodent and nonhuman primate brains using the high affinity radioligand, 18F-fallypride. *Nuclear Medicine and Biology*. 26:519-527.
8. Narendran R, Slifstein M, Guillin O, Hwang Y, Hwang D-R, Scher E, et al. (2006): Dopamine (D2/3) receptor agonist Positron Emission Tomography radiotracer [11C]-(+)-PHNO is a D3 receptor preferring agonist in vivo *Synapse*. 60:485-495.
9. Martin GE, Williams M, Pettibone DJ, Yarbrough GG, Clineschmidt BV, Jones JH (1984): Pharmacologic profile of a novel potent direct-acting dopamine agonist, (+)-4-propyl-9-hydroxynaphthoxazine [(+)-PHNO]. *J Pharmacol Exp Ther*. 230:569-576.
10. Wilson AA, McCormick P, Kapur S, Willeit M, Garcia A, Hussey D, et al. (2005): Radiosynthesis and evaluation of [11C]-(+)-4-propyl-3,4,4a,5,6,10b-hexahydro-2H-naphtho[1,2-b][1,4]oxazin-9 -ol as a potential radiotracer for in vivo imaging of the dopamine D2 high-affinity state with positron emission tomography. *J Med Chem*. 48:4153-4160.
11. Willeit M, Ginovart N, Kapur S, Houle S, Hussey D, Seeman P, et al. (2006): High-Affinity States of Human Brain Dopamine D2/3 Receptors Imaged by the Agonist [11C]-(+)-PHNO. *Biological Psychiatry*. 59:389-394.
12. Rabiner EA, Slifstein M, Nobrega J, Plisson C, Huiban M, Raymond R, et al. (2009): In vivo quantification of regional dopamine-D3 receptor binding potential of (+)-PHNO: Studies in non-human primates and transgenic mice. *Synapse*. 63:782-793.
13. PCT International Publication WO2005/080382 poS, entitled "Azabicyclo (3.1.0) hexane derivatives useful as modulators of dopamine receptors".
14. Martinez D, Mawlawi O, Simpson N, Hwang D, Kegeles L, Broft A (2000): Comparison of amphetamine-induced endogenous dopamine release in striatal substructures in humans using PET. . *Soc Neurosc Abst*
15. Seeman P, Grigoriadis DE (1987): Dopamine receptors in brain and periphery. *Neurochemistry international*. 10:1-25.
16. Sibley DR, De Lean A, Creese I (1982): Anterior pituitary dopamine receptors. Demonstration of interconvertible high and low affinity states of the D-2 dopamine receptor. *Journal of Biological Chemistry*. 257:6351-6361.
17. Zahniser NR, Molinoff PB (1978): Effect of guanine nucleotides on striatal dopamine receptors. *Nature*. 275:453-455.
18. Lammertsma AA, Hume SP (1996): Simplified Reference Tissue Model for PET Receptor Studies. *NeuroImage*. 4:153-158.

19. Gunn RN, Lammertsma AA, Hume SP, Cunningham VJ (1997): Parametric Imaging of Ligand-Receptor Binding in PET Using a Simplified Reference Region Model. *NeuroImage*. 6:279-2787.
20. Slifstein M, Parsey RV, Laruelle M (2000): Derivation of [11C]WAY-100635 binding parameters with reference tissue models: effect of violations of model assumptions. *Nuclear Medicine and Biology*. 27:487-492.
21. Ginovart N, Willeit M, Rusjan P, Graff A, Bloomfield PM, Houle S, et al. (2007): Positron emission tomography quantification of [11C]PHNO binding in the human brain. *J Cereb Blood Flow Metab*. 27:857-871.
22. Boileau I, Guttman M, Rusjan P, Adams JR, Houle S, Tong J, et al. (2009): Decreased binding of the D3 dopamine receptor-preferring ligand [11C]-(+)-PHNO in drug-naive Parkinson's disease. *Brain*. 132:1366-1375.
23. Graff-Guerrero A, Redden L, Abi-Saab W, Katz DA, Houle S, Barsoum P, et al. (2009): Blockade of [11C](+)-PHNO binding in human subjects by the dopamine D3 receptor antagonist ABT-925. *The International Journal of Neuropsychopharmacology*. First View:1-15.
24. Graff-Guerrero A, Mizrahi R, Agid O, Marcon H, Barsoum P, Rusjan P, et al. (2008): The Dopamine D2 Receptors in High-Affinity State and D3 Receptors in Schizophrenia: A Clinical [11C]-(+)-PHNO PET Study. *Neuropsychopharmacology*. 34:1078-1086.
25. Murray AM, Ryoo HL, Gurevich E, Joyce JN (1994): Localization of dopamine D3 receptors to mesolimbic and D2 receptors to mesostriatal regions of human forebrain. *Proc Nat Acad Sci USA*. 91:11271-11275.
26. Seeman P, Wilson A, Gmeiner P, Kapur S (2006): Dopamine D2 and D3 receptors in human putamen, caudate nucleus, and globus pallidus. *Synapse*. 60:205-211.
27. Gurevich EV, Joyce JN (1999): Distribution of Dopamine D3 receptor expressing neurons in the human forebrain comparison with D2 receptor expressing neurons. *Neuropsychopharmacology*. 20:60 - 80.
28. Graff-Guerrero A, Mamo D, Shammi CM, Mizrahi R, Marcon H, Barsoum P, et al. (2009): The Effect of Antipsychotics on the High-Affinity State of D2 and D3 Receptors: A Positron Emission Tomography Study With [11C]-(+)-PHNO. *Arch Gen Psychiatry*. 66:606-615.
29. Quik M, Police S, He L, Di Monte DA, Langston JW (2000): Expression of D3 receptor messenger RNA and binding sites in monkey striatum and substantia nigra after nigrostriatal degeneration: effect of levodopa treatment. *Neuroscience*. 98:263-273.
30. Stanwood GD, Artymyshyn RP, Kung M-P, Kung HF, Lucki I, McGonigle P (2000): Quantitative Autoradiographic Mapping of Rat Brain Dopamine D3 Binding with [125I]7-OH-PIPAT: Evidence for the Presence of D3 Receptors on Dopaminergic and Nondopaminergic Cell Bodies and Terminals. *Journal of Pharmacology and Experimental Therapeutics*. 295:1223-1231.
31. Gallezot J-D, Beaver J, Nabulsi N, Weinzimmer D, Slifstein M, Gunn RN, et al. (2009): [11C]PHNO Studies in Rhesus Monkey: In vivo Affinity for D2 and D3 Receptors and Dosimetry. *Society for Nuclear Medicine Annual Meeting*. Toronto.
32. Rabiner E, Slifstein M, Gunn RN, Gentile G, Xu X, Huibain M (2008): D3 receptor assessment in vivo: PET with [11C]PHNO and SB277011. *Society for Nuclear Medicine Annual Meeting*. New Orleans.
33. Gurevich E, Bordelon Y, Shapiro R, Arnold S, Gur R, Joyce J (1997): Mesolimbic dopamine D-3 receptors and use of antipsychotics in patients with schizophrenia - A postmortem study. *Arch Gen Psychiatry* 54:225-232.
34. Volkow ND, Fowler JS, Wang G-J, Swanson JM, Telang F (2007): Dopamine in Drug Abuse and Addiction: Results of Imaging Studies and Treatment Implications. *Arch Neurol*. 64:1575-1579.

Table 1. Estimated binding of [^{11}C]-(+)-PHNO to D3 and D2HIGH receptors in the human brain

Parameter (unitless)	Regions					
	SN	GP	VST	THA	DCA	DPU
f_{PHNO}^{D3}	1.00 (0.79-1.00)	0.67 (0.55-0.80)	0.26 (0.18-0.35)	0.46 (0.00-1.00)	0.01 (0-0.14)	0.00 (0.00-0.11)
BP_{ND}	1.39 (1.28-1.49)	2.83 (2.72-2.93)	2.94 (2.83-3.04)	0.39 (0.28-0.49)	1.85 (1.75-1.95)	2.37 (2.26-2.47)
BP_{ND}^{D3}	1.39	1.90	0.77	0.18	0.02	0.00
BP_{ND}^{D2HIGH}	0.00	0.92	2.16	0.21	1.83	2.37

Parameters estimated using the model described in Equation 5b: fraction of baseline [^{11}C]-(+)-PHNO BP_{ND} corresponding to binding to D3 receptors (f_{PHNO}^{D3}), total baseline [^{11}C]-(+)-PHNO BP_{ND} and baseline [^{11}C]-(+)-PHNO BP_{ND} to D3 (BP_{ND}^{D3}) and D2HIGH (BP_{ND}^{D2HIGH}) receptor sites in various regions of the human brain (substantia nigra, SN; globus pallidus, GP; ventral striatum, VST; thalamus, THA; dorsal caudate, DCA; dorsal putamen, DPU). The values for BP_{ND}^{D3} and BP_{ND}^{D2HIGH} were calculated directly from the model parameters f_{PHNO}^{D3} and BP_{ND} which were fitted to the data acquired. Values in parentheses represent 95% confidence intervals.

Table 2. Comparison of [^{11}C]-(+)-PHNO in vivo pharmacological studies.

Species	Agent	Source	SN	GP	VST	THA	DCA	DPU
Baboon	BP897	(8)	90%	57%	30%	60%	13%	13%
Baboon	SB27011	(12)	100%	72%	49%	82%	23%	8%
Baboon	GSK598809	Unpublished data	90%	89%	58%	97%	22%	4%
Human	GSK598809	This study	100%	67%	26%	46%	1%	0%
Human	ABT925	(23)	100%	90%	62%	-	55%	53%

Fraction of [^{11}C]-(+)-PHNO BP_{ND} displaceable by putative D3 receptor selective agents, in baboons and humans, in various brain regions (substantia nigra, SN; globus pallidus, GP; ventral striatum, VST; thalamus, THA; dorsal caudate, DCA; dorsal putamen, DPU) in baboons and human studies. * Value for dorsal striatum. -, not reported. See text for doses.

FIGURE LEGENDS

Figure 1. Baseline [^{11}C]-(+)-PHNO integral images (summed over 10-90 min.) (top row) and associated MR image (bottom row) in one representative subject. Sections on the left were selected to show the substantia nigra (SN) region. Sections on the right show dorsal caudate (DCA), dorsal putamen (DPU), ventral striatum, (VST) globus pallidus (GP) and thalamus (THA).

Figure 2. [^{11}C]-(+)-PHNO time activity curves and SRTM model fits in one subject at baseline (top) and after oral administration of 175 mg of GSK598809 (bottom) showing cerebellum, CER; substantia nigra, SN; globus pallidus, GP; ventral striatum, VST; thalamus, THA; dorsal caudate, DCA; dorsal putamen, DPU. At baseline, regions of highest uptake include the three striatal regions (VST, DCA, DPU), GP and SN, while THA activity is only marginally higher than CER. CER, THA and the three striatal regions (VST, DCA,DPU) display early peaks followed by rapid wash-out. In GP and SN, the wash-out rate is more protracted. Following 175 mg GSK598809, SN uptake decreased to the CER levels, GP was reduced, and striatal regions were only mildly affected.

Figure 3. Mean ± SD of measured [^{11}C]-(+)-PHNO BP_{ND} in six ROIs during baseline scans (n = 19). Legend: substantia nigra, SN; globus pallidus, GP; ventral striatum, VST; thalamus, THA; dorsal caudate, DCA; dorsal putamen, DPU.

Figure 4. [^{11}C]-(+)-PHNO integral images (summed over 10-90 min.) at baseline (top row) and after administration of 175 mg GSK598809 (bottom row). Slices are selected to illustrate the marked change in SN, moderate change in GP and VST, and marginal change in dorsal striatal regions.

Figure 5. Plots of [^{11}C]-(+)-PHNO displacement against plasma concentration of GSK598809 in six brain regions. Solid lines represent model fits (via Equation 5) to the measured data. Legend: substantia nigra, SN; globus pallidus, GP; ventral striatum, VST; thalamus, THA; dorsal caudate, DCA; dorsal putamen, DPU. The asymptotes of the curves provided f_{PHNO}^{D3}. At high concentrations, GSK598809 almost completely blocked the specific binding of [^{11}C]-(+)-PHNO in SN, with negligible effects on the DCA and DPU.

Figure 6. Measured baseline [^{11}C]-(+)-PHNO BP_{ND} divided into portions corresponding to D_3

receptors (BP_{ND}^{D3} , black area) and D_{2HIGH} receptor (BP_{ND}^{D2HIGH} , grey area) by regions. BP_{ND}^{D3} obtained by multiplying [^{11}C]-(+)-PHNO BP_{ND} by f_{PHNO}^{D3} , BP_{ND}^{D2HIGH} obtained as BP_{ND} minus BP_{ND}^{D3} . Legend: substantia nigra, SN; globus pallidus, GP; ventral striatum, VST; thalamus, THA; dorsal caudate, DCA; dorsal putamen, DPU.

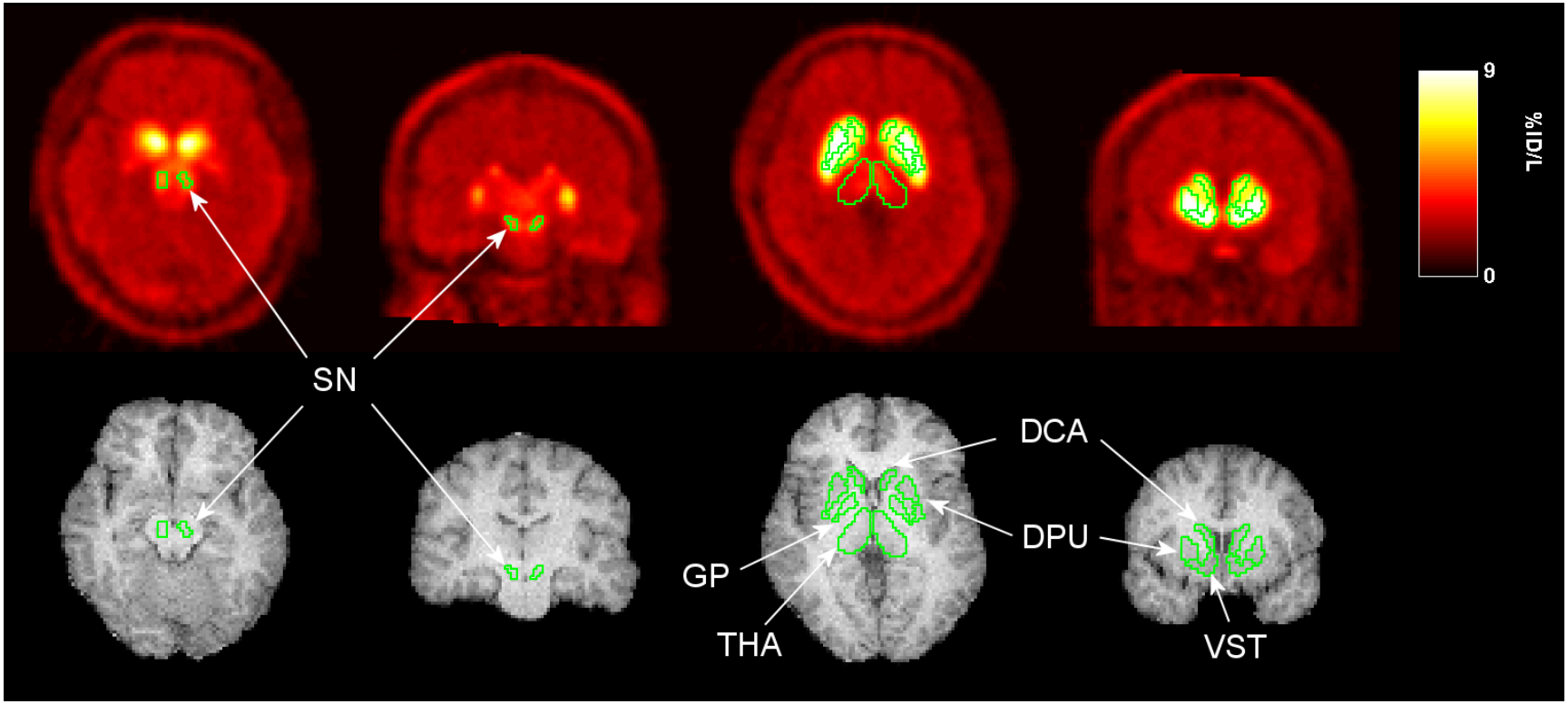

Figure 1

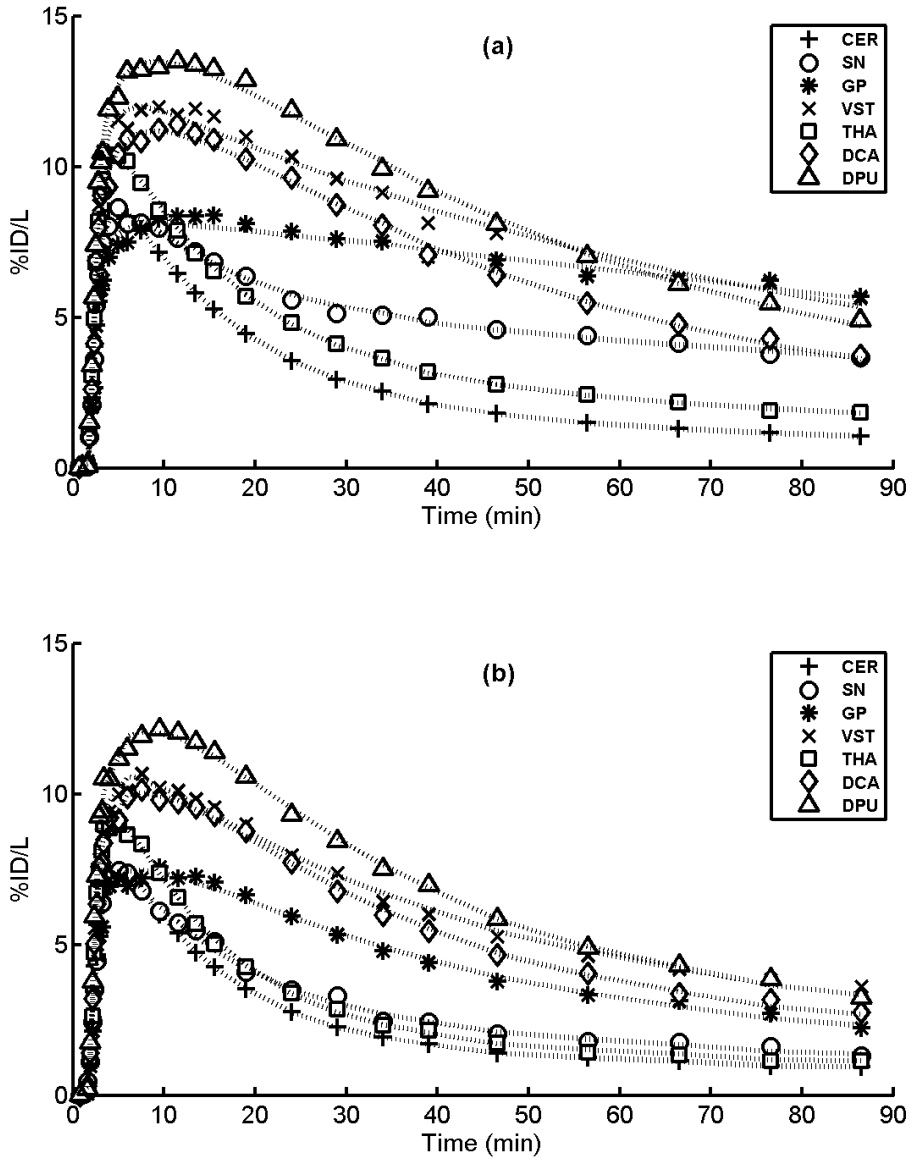
(a)
CER
SN
GP
VST
THA
DCA
DPU
%ID/L
Time (min)
(b)
CER
SN
GP
VST
THA
DCA
DPU
%ID/L
Time (min)

Figure 2

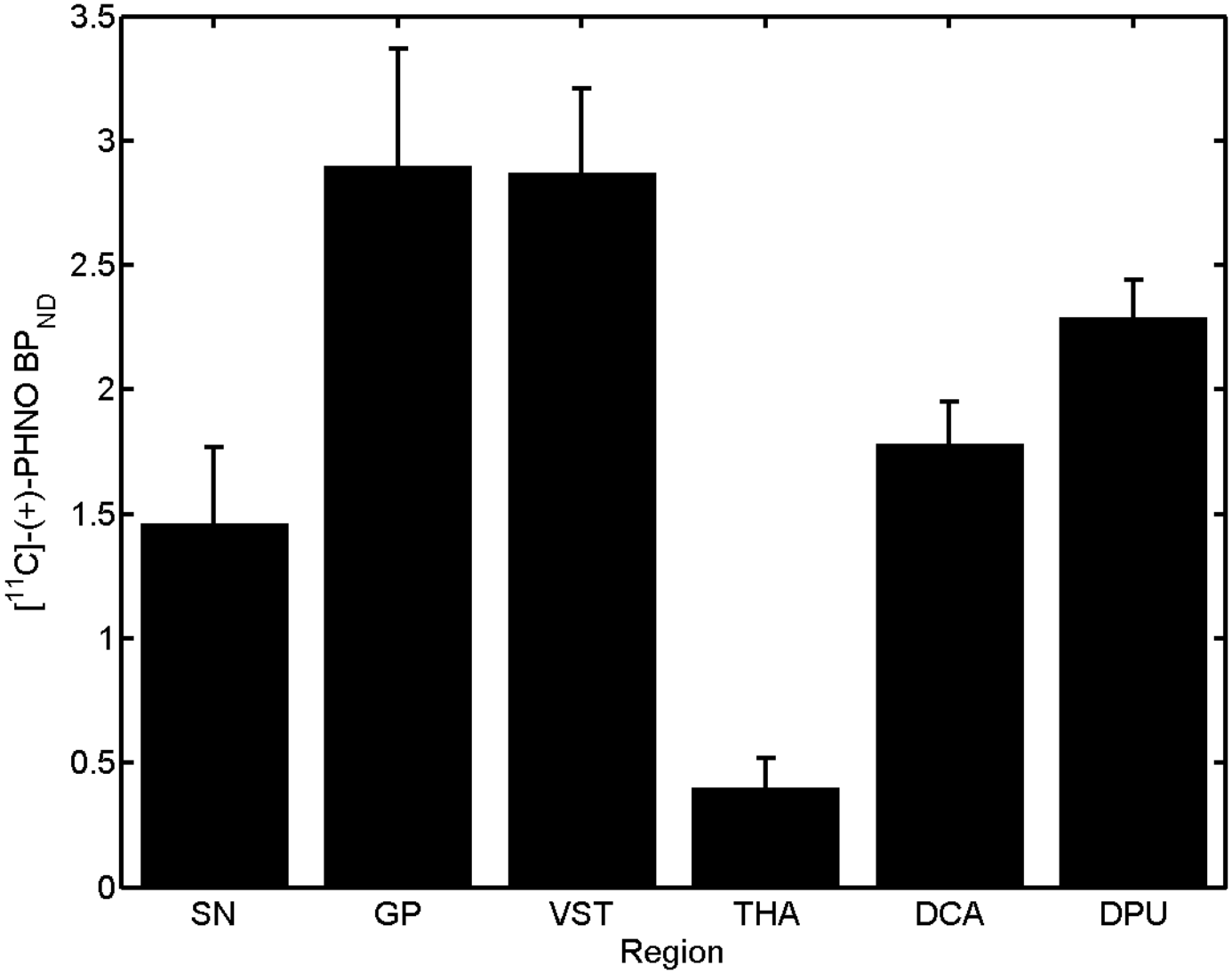

Figure 3

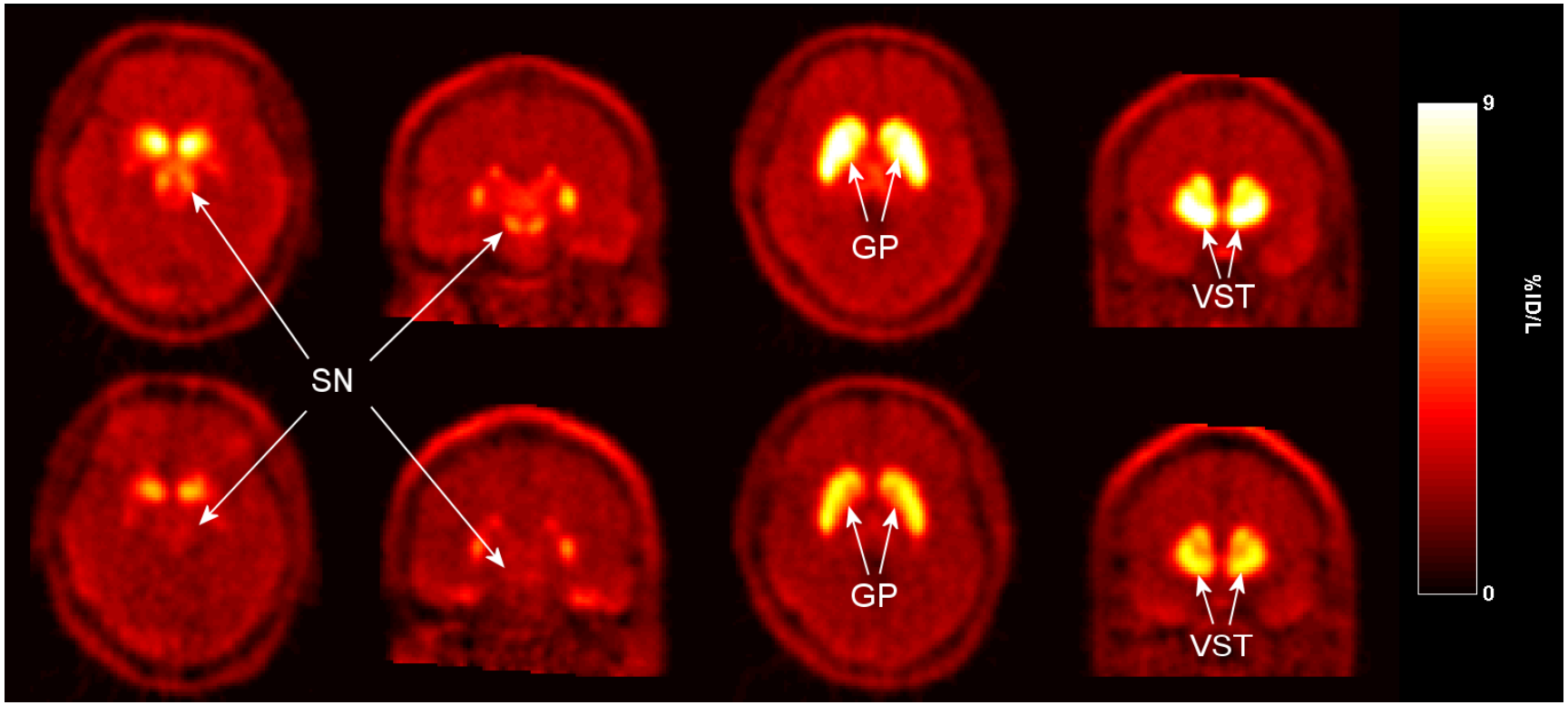

Figure 4

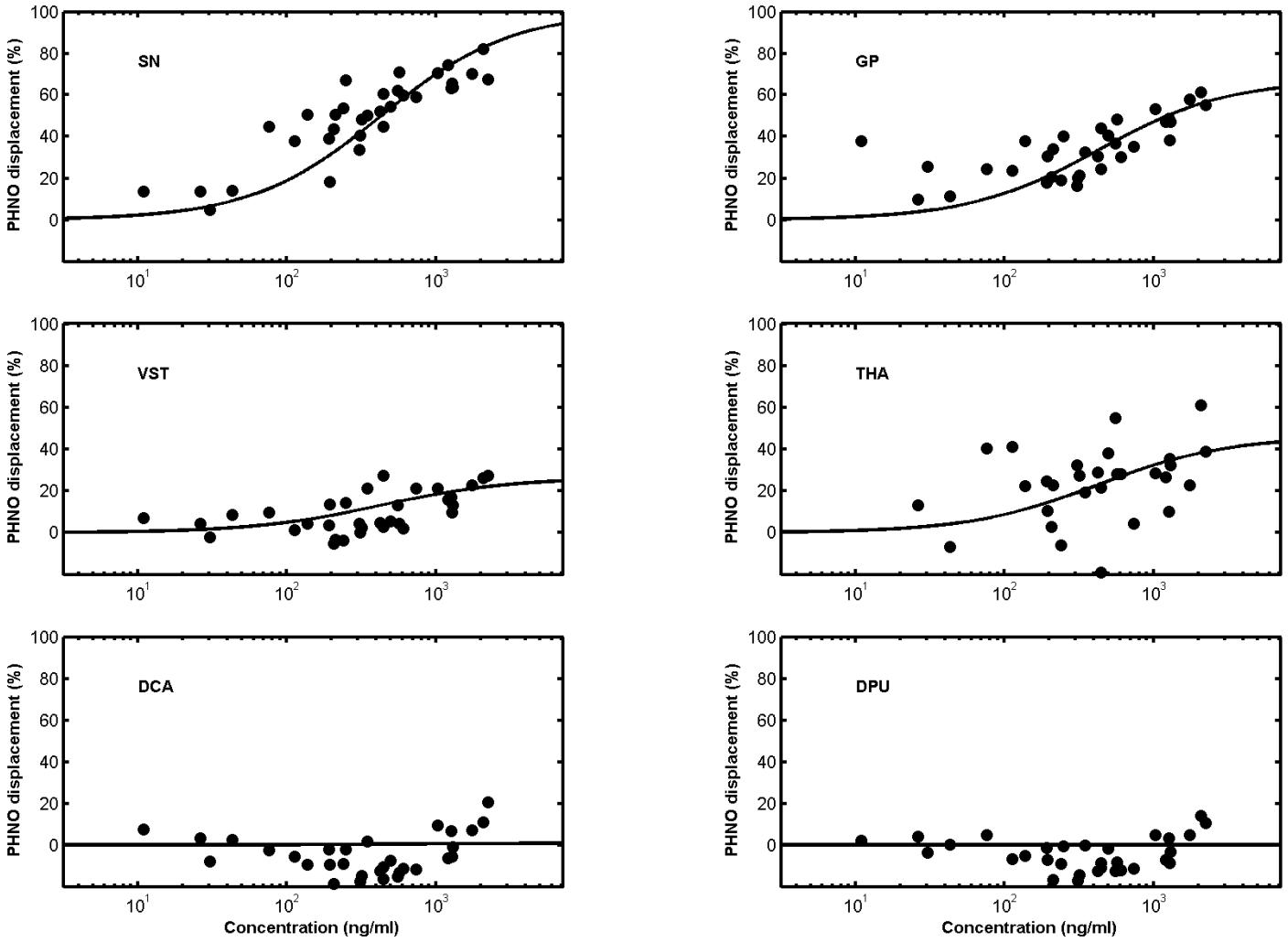
SN
GP
VST
THA
DCA
DPU
PHNO displacement (%)
Concentration (ng/ml)
0
20
40
60
80
100
10^1
10^2
10^3

Figure 5

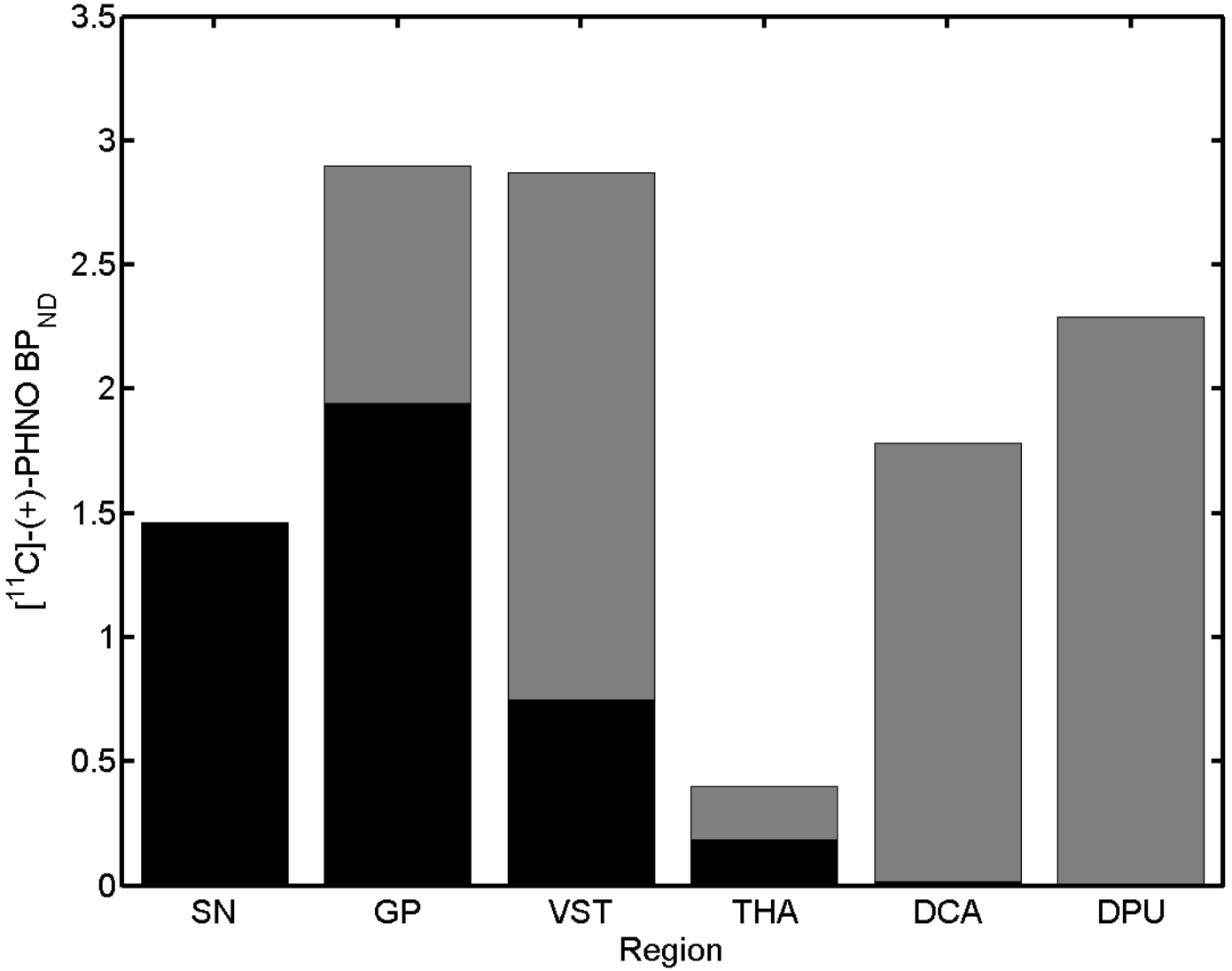

Figure 6